



Research paper

Exogenic production of bioactive filamentous biopolymer by monogonant rotifers

Zsolt Datki^{a,*}, Eva Acs^{b,c,1}, Evelin Balazs^a, Tamas Sovany^d, Ildiko Csoka^d, Katalin Zsuga^e, Janos Kalman^a, Zita Galik-Olah^a

^a Department of Psychiatry, Faculty of Medicine, University of Szeged, Vasas Szent Peter u. 1-3, H-6724 Szeged, Hungary

^b Danube Research Institute, MTA Centre for Ecological Research, Karolina ut 29-31, H-1113 Budapest, Hungary

^c National University of Public Service, Faculty of Water Sciences, 6500 Baja, Bajcsy-Zsilinszky utca 12-14., Hungary

^d Institute of Pharmaceutical Technology and Regulatory Affairs, Faculty of Pharmacology, University of Szeged, Eotvos u. 6, H-6720 Szeged, Hungary

^e Agrint Kft., Facan sor 56, H-2100 Godollo, Hungary



ARTICLE INFO

Edited by Professor Bing Yan

Keywords:

Monogonant rotifer

Biopolymer

Euchlanis dilatata

SH-SY5Y neuroblastoma cell line

Exudate

Beta-amyloid

Chemical compounds studied in this article:

Acetic acid (PubChem CID: 176)

Beta-amyloid 1-42 (PubChem CID: 57339251)

BSA (PubChem CID: 384256260)

Calcein-AM (PubChem CID: 390986)

Carmine crystals (PubChem CID: 14950)

Collagenase II (PubChem CID: 18680304)

DMSO (PubChem CID: 679)

EDTA (PubChem CID: 6049)

EGTA (PubChem CID: 6207)

Ethanol (PubChem CID: 702)

Glycerol (PubChem CID: 753)

HCl (PubChem CID: 313)

KBr (PubChem CID: 253877)

Micro-cellulose (PubChem CID: 16211032)

Methanol (PubChem CID: 887)

NaHCO₃ (PubChem CID: 516892)

NaN₃ (PubChem CID: 335587)

NaOH (PubChem CID: 14798)

SDS (PubChem CID: 8778)

Spermidine (PubChem CID: 1102)

ABSTRACT

The chemical ecology of rotifers has been little studied. A yet unknown property is presented within some monogonant rotifers, namely the ability to produce an exogenic filamentous biopolymer, named 'Rotimer'. This rotifer-specific viscoelastic fiber was observed in six different freshwater monogonants (*Euchlanis dilatata*, *Lecane bulla*, *Lepadella patella*, *Itura aurita*, *Colurella adriatica* and *Trichocerca iernis*) in exception of four species. Induction of Rotimer secretion can only be achieved by mechanically irritating rotifer ciliate with administering different types (yeast cell skeleton, denatured BSA, epoxy, Carmine or urea crystals and micro-cellulose) and sizes (approx. from 2.5 to 50 μm diameter) of inert particles, as inductors or visualization by adhering particles. The thickness of this Rotimer is 33 ± 3 nm, detected by scanning electron microscope. This material has two structural formations (fiber or glue-like) in nano dimension. The existence of the novel adherent natural product becomes visible by forming a 'Rotimer-Inductor Conglomerate' (RIC) web structure within a few minutes. The RIC-producing capacity of animals, depends on viability, is significantly modified according to physiological (depletion), drug- (toxin or stimulator) and environmental (temperature, salt content and pH) effects. The *E. dilatata*-produced RIC is affected by protein disruptors but is resistant to several chemical influences and its Rotimer component has an overwhelming cell (algae, yeast and human neuroblastoma) motility inhibitory effect, associated with low toxicity. This biopolymer-secretion-capacity is protective of rotifers against human-type beta-amyloid aggregates.

Abbreviations: ASC, Average Size of Conglomerates; ASIP, Average Size of Inductor Particles; Aβ42, Beta-amyloid 1-42; BSA, bovine serum albumin; CA, Covered Area; DW, distilled water; DMSO, dimethyl sulfoxide; EDTA, ethylenediaminetetraacetic acid; EGTA, ethylene glycol-bis(β-aminoethyl ether)-N,N,N',N'-tetraacetic acid tetrasodium salt; EtOH, ethanol; FI, fluorescence intensity; FTIR, Fourier Transform Infrared Spectroscopy; NaN₃, sodium azide; NaOH, sodium hydroxide; NR, Number of Rotifers; MeOH, methanol; RIC, Rotimer-Inductor Conglomerate; RPC, RIC-producing capacity; RPC_i, RPC index; SEM, scanning electron microscope; S.E.M., standard error of the mean; SDS, sodium dodecyl sulfate; TPEN, N,N,N',N'-Tetrakis(2-pyridylmethyl)ethylenediamine.

* Corresponding author.

E-mail addresses: datki.zsolt@med.u-szeged.hu, datkizsolt@gmail.com (Z. Datki).

¹ First co-authors

<https://doi.org/10.1016/j.ecoenv.2020.111666>

Received 2 September 2020; Received in revised form 31 October 2020; Accepted 12 November 2020

Available online 21 November 2020

0147-6513/© 2020 The Author(s). Published by Elsevier Inc. This is an open access article under the CC BY license (<http://creativecommons.org/licenses/by/4.0/>).

TPEN (PubChem CID: 5519)
 Triton X-100 (PubChem CID: 5590)
 Trypsin (PubChem CID: 5311489)
 Urea (PubChem CID: 1176)

1. Introduction

Rotifers are multicellular animals of microscopic size, providing a significant part of aquatic biomass (Dahms et al., 2011). Both bdelloids and monogonants are found in marine environment or in freshwater lakes (Snell et al., 2015). Although their bodies consist of approximately 1000 cells, they have complex organ systems, including gastro-intestinal tract, reproductive organs, nervous system or secretory glands. These entities are excellent models of ecotoxicology, aging or pharmaceutical researches (Datki et al., 2018, 2019; Snell et al., 2018; Macsai et al., 2019).

Self-maintenance and the reproductive rate are the two most important factors of these microinvertebrates during their lifespan, and in their natural habitat the general nutrients include degradable organic masses (Fontaneto et al., 2011; Robeson et al., 2011). Rotifers are able to use conglomerates and aggregates as 'food' by their phylogenetically selected ability. Bdelloids, such as *Philodina acuticornis* or *Adineta steineri*, are able to exceedingly catabolize the highly enzyme-resistant human-type neurotoxic aggregates, such as beta-amyloid, alpha-synuclein and scrapie-type prion under certain extreme conditions (e.g. starvation; Datki et al., 2018). Another example for invertebrate adaptive capacity is the secretion of various types of biopolymers, especially in marine species belonging to the phylum of *Mollusca*, *Echinodermata* or *Arthropoda* (Ganesana et al., 2020).

Biopolymers are produced by living organisms and these chemical substances consist of repetitive units, which form molecular structures of higher order. Based on their chemical properties, several types of natural products can be distinguished: polypeptides, polynucleotides, polysaccharides, peptidoglycans, proteoglycans, glycoproteins and the mixed types of these groups. (Chandra and Rustgi, 1998; Hassan et al., 2019) Their enzyme resistance or sensitivity strongly correlates with their basic structure, for example, polypeptides can be degraded by proteases, such as trypsin or proteinase K (Muhlia-Almazán et al., 2008). The biopolymers, showing specific antimicrobial (Kamiya et al., 2006; Rahman, 2019) or hypoglycemic activities (Ruiz-Torres et al., 2019), are used in multiple fields for pharmaceutical (Yavuz et al., 2019), medical (Humenik et al., 2019) or industrial purposes (Chen and Peng, 2019; Mohamed et al., 2020). The original function of these natural products are various, depending on the lifestyle and environment of relevant animals, e.g. the sessile marine invertebrates (mussels, tubeworm, sea star, limpet, sea cucumber) produce bioadhesives to attach to different surfaces. The adhesive capability depends on the various types of attachment which can be permanent, transitory, temporary and instantaneous. (Hennebert et al., 2018) One of the earliest adhesive biopolymers is described by Aristotle, called *byssus*, which is produced by a marine mollusc, *Pinna nobilis*. This substance is barely studied in the fields of biochemistry, material science, biomedicines and biomimetics. At the southern part of Europe and North Africa this fibrous and shock-absorbing biopolymer was used in textile manufacturing due to its fine, but very resilient structure. There are species-specific differences between the chemical and structural forms of these exudates, but their common characteristics include self-healing, stiffness, bio-renewable and DOPA-dependent adhesive abilities. Their chemical structures predominantly contain protein with minor amounts of lipids and carbohydrates. These substances are characterized by comprehensive flexibility, ability to fast recovery and high biomimetic potential. Being dissimilar to other typical elastomeric proteins, they provide novel tools for medico-industrial developments. In many cases, the clear chemical definition, the biochemistry and the genomics of these biopolymers

remain to be enigmatic. For example, the exact structure of *Gorgonin* (a protein-based polyphenol-containing organic material), which was first described by Pallas (1766), is still unknown (Ehrlich, 2019; Olatunji, 2020).

Since the marine invertebrates adapt to ecological niche, their host defense system is completely different from that of the terrestrial ones. Certain species secrete antibacterial and antitumor factors; furthermore, others produce bioactive factors with the same properties, but with different chemical structures. (Yamazaki et al., 1985, 1989; Kisugi et al., 1992;) No relevant data were found about the biopolymer-secretion of monogonant or bdelloid rotifers. The complex biodiversity of rotifers is dealt with a growing number of studies that intend to reveal the physiology of these invertebrates, still having new properties or phenomena to be explored. A yet unknown capability of monogonants were aimed to describe, understanding how the environmental and chemical factors influence the newly observed rotifer-specific biopolymer secretion, stability and bioactivity. Furthermore, some examples were intended to be shown to demonstrate the potential application of this recently described natural product.

2. Material and methods

2.1. Materials

Materials applied in this work were the followings: yeast (*Saccharomyces cerevisiae*; EU-standard granulated instant form, cat. no.: 2-01-420674/001-Z12180/HU); algae (*Chlorella vulgaris*; BioMenu, Caleido IT-Outsource Kft.; cat. no.:18255); from Sigma-Aldrich: bovine serum albumin (BSA; cat. no.: A-9418); sodium spermidine (cat. no.: S2626), Calcein-AM (cat. no.: 17783), Proteinase K (cat. no.: P-6556), Potassium bromide (cat. no.: 221864), Triton X-100 (cat. no.: X-100), dimethyl sulfoxide (DMSO; cat. no.: D8418), ethylenediaminetetraacetic acid (EDTA; cat. no.: E9884), ethylene glycol-bis(β -aminoethyl ether)-N,N,N',N'-tetraacetic acid tetrasodium salt (EGTA; cat. no.: E8145), N,N,N',N'-Tetrakis(2-pyridylmethyl)ethylenediamine (TPEN; cat. no.: P4413), acetic acid (cat. no.: 695092), Whatman filter (pore diameter: 2 μ m; cat. no.: 6783-2520), SH-SY5Y human neuroblastoma cell line (cat. no.: 94030304); from Merck: powdered Carmine crystals (Natural Red 4; cat. no.: 2233), sodium azide (NaN₃; cat. no.: 822335), methanol (MeOH; cat. no.: 1.07018.2511), glycerol (cat. no.: 1.04092.1000), hydrochloric acid (HCl; cat. no.: 1.00317.1000), distilled water (DW; Millipore Ultrapure); Dynabeads M-270 epoxy (Life Technologies AS, cat. no.: 14301); from Reanal: sodium dodecyl sulfate (SDS; cat. no.: 24680-1-0833), sodium hydroxide (NaOH; cat. no.: 24578-1-01-38), urea crystals (cat. no.: 08072), micro-cellulose (cat. no.: D-76); from Biochrom HG: trypsin (Seromed, cat. no.: L2103), Collagenase II (Seromed; Worthington, 252 U/mg; cat. no.: L6723); from Corning or Corning-Costar: 24-well plate (cat. no.: 3524), 96-well plate (Nunc; cat. no.: 167008), Petri dish (cat. no.: 430167), flasks (cat. no.: 430168); universal plastic web (pore diameters: 15 and 50 μ m); ethanol (EtOH; Molar Chemicals Kft.; cat. no.: 02911-481-430); standard medium (mg/L): Ca²⁺ 31.05; Mg²⁺ 17.6; Na⁺ 0.9; K⁺ 0.25; Fe²⁺ 0.001; HCO₃⁻ 153.097; SO₄²⁻ 3; Cl⁻ 0.8; F⁻ 0.02; H₂SiO₃ 3.3 (pH = 7.5), elevated salt medium (standard medium supplemented with 790 mg/L NaHCO₃). The glass coverslip (diameter: 12 mm, thickness: 0.15 mm; cat. no.: 89167-106) was obtained from VWR International, Houston. The beta-amyloid 1-42 (A β 42; cat. no.: A14075, human Amyloid b-Peptide 1-42; 107761-42-2) was purchased from AdooQ Bioscience LLC., California.

2.2. Harvesting and identification of different rotifer species

To collect and isolate different monogonant rotifers, the method described by Debortoli et al. (2016) was used with minor modifications. Source of samples was located in the Red Cross Lake (Vértó; 27,000 m²; GPS coordinates: 46° 16' 25" N; 20° 08' 39" E; early summer) in Szeged (Southern Great Plain, Hungary). The original media of collected samples were substituted with standard medium in separate Petri dishes. The species collected were *Euchlanis dilatata*, Ehrenberg, 1832; *Lecane bulla*, Gosse, 1851; *Lepadella patella*, O. F. Muller, 1773; *Itura aurita*, Ehrenberg, 1830; *Colurella adriatica*, Ehrenberg, 1831; *Trichocerca iernis*, Gosse, 1887; *Cephalodella intuta*, Myers, 1924; *Brachionus leydigii rotundus*, Rousselet, 1907; *Brachionus calyciflorus*, Pallas, 1766; *Synchaeta pectinata*, Ehrenberg, 1832 which were photographed (Nikon D5100, DSLR, RAW-NEF, 16 MP, ISO 100; Nikon Corp., Kanagawa, Japan) under inverted light microscope (at 63X and 400X magnification; Leitz Labovet, Wetzlar, Germany). Serial images were taken at every 5- μ m intervals yielding a total of 5–8 photographic layers per rotifer, which were subsequently merged into one superimposed picture (by using Photoshop CS3 software, Adobe Systems Inc., San Jose) to achieve better resolution. The entities were paralyzed with carboxygenated (5% CO₂) standard medium for 5 min during photo recordings. After the species were identified based on methods described in academic literature (Kertész, 1894; Kutikova, 1970; Koste, 1978; Nogrady and Segers, 2002; Varga, 1966), species-specific information (e.g., body size in relation to age) was applied to collect relatively mature individuals (generally with an egg in their body). Animals were collected and isolated (using a micropipette) to create separated and monoclonal populations. After completing the experiments, *E. dilatata*, *L. bulla* and *C. intuta* were maintained as standard cultures of our laboratory.

2.3. In vivo and in vitro culturing

All investigated rotifers (Fig. 1A–J) were cultured in flasks (25 cm² area) filled with standard medium. They were fed every second day by heat-inactivated, homogenized and filtered (plastic web; pore diameter: 15 μ m) algae-yeast (in 1:3 ratio) suspension (final dose: 600 μ g/mL/case). The live algae- and yeast cell cultures, to carry out viability experiments, were started with rehydration in glucose supplemented (1 mM) standard medium left to rest for 16 h at room temperature.

For in vitro measurements, the popular adrenergic SH-SY5Y human

neuroblastoma cell line was applied with the related culturing entirely based on the previous works of Datki et al., (2003, 2018).

2.4. Exudate-inductions and adequate targeted treatments

The experimental animals were isolated by pouring them into Petri dishes (55 cm² area). In all rotifer-specific biopolymer (named 'Rotimer') related experiments, 20 mature animals (with an egg inside or with maximal body size) were applied per well in a 24-well plate (1.8 cm² area) with 1 mL working volume.

The final (working) concentration of the administered inductors of Rotimer-secretion was 50 μ g/mL, diluted from 1 mg/mL stock solution. Every inductor (Table 1) was prepared in line with their own molecular properties: a. yeast: heat inactivated cell skeleton; b. BSA: heat denatured (den-BSA; 20 min, 80 °C, in DW); c. epoxy: metal beads coated with polymers; d. Carmine: mechanically ultra-powdered dye crystals (with classic electric coffee grinder); e. urea: ultra-powdered crystals; f. cellulose: powdered micro-cellulose.

To lose the non-specific adhesion of inductors to well-surface, the medium (without rotifer and Rotimer), containing particles, was decanted from the wells, and the passively covered area was maximum 1% in these blank (rotifers-free) experiments. Secretion of particle-induced biopolymer resulted a 'Rotimer-inductor conglomerate' (RIC) in a high density web form after 20 min incubation time (Fig. 1K–M; with yeast inductor). After carefully removing the well solution, these RIC products were desiccated (dried) at room temperature (25 °C) and at 40% humidity in the dark for 30 min. This preparation method was also administered in high resolution, monitoring the Rotimer fibers and gluelike format (Fig. 1L; with epoxy inductor). The inductor particles were applied under the size of 2 μ m (the Carmine inductor was filtered with Whatman filter) or above 50 μ m (filtered with plastic web) where they were unable to induce the Rotimer secretion and RIC formation. The RIC patterns, detected by light microscopy, were photographed (Nikon D5100) and the pictures were converted in a black and white graphical format (threshold; 2.04 pixel = 1 μ m; 8-bit). These images were analyzed with ImageJ program (Wayne Rasband, USA), extracting data related to the conglomerate-covered area (%) and the average size (μ m²) of this complex. RIC analysis was used to select the higher RIC-producing species using the yeast inductor (Fig. 2A) related to RIC-producing capacity (RPC; Suppl. Video); furthermore, the RPC was also applied for screening different Rotimer inductors (Fig. 2B) and

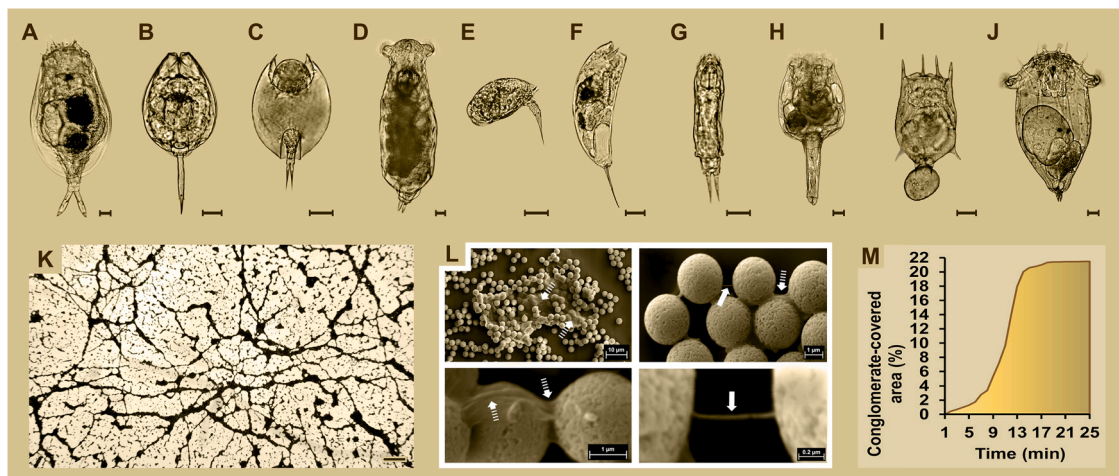


Fig. 1. Presentation of rotifers and their specific biopolymer (Rotimer) by its conglomerates. The representative photos of monogonant rotifer species (A–F) are shown. The monitored species in Rotimer-related experiments (scale bar: 20 μ m) are the followings: *Euchlanis dilatata* (A), *Lecane bulla* (B), *Lepadella patella* (C), *Itura aurita* (D), *Colurella adriatica* (E), *Trichocerca iernis* (F), *Cephalodella intuta* (G), *Brachionus leydigii rotundus* (H), *Brachionus calyciflorus* (I), *Synchaeta pectinata* (J). The picture shows the web of 'Rotimer-Inductor Conglomerate' (RIC) which was formed by *E. dilatata* (K; scale bar: 200 μ m). The montage of representative photos of SEM (L) show the different types of Rotimer after epoxy induction (scale bars 0.2 and 1 μ m). The filamentous form is indicated by arrows and the gluelike structure is presented by dashed arrows. Exponential kinetic of RIC formation (M) was measured by time-dependent (min) saturation of the conglomerate-covered area (%).

Table 1
Outline of basi experimental runs.

Experiments	Monogonant species	Applied inductors	Treatment agents or environment	Test entities, cells or targets	Measured parameters	Visualisation methods
Presentation of rotifers and their specific biopolymer (Rotimer) by its conglomerates. (Fig. 1)	<i>E. dilatata</i>	yeast epoxy	standard medium	<i>E. dilatata</i>	conglomerate-covered area fiber and glue-like form	light microscopy scanning electron microscopy
Rotifer-specific production of Rotimer-Inductor Conglomerates (RIC) (Fig. 2A)	<i>E. dilatata</i> <i>L. bulla</i> <i>L. patella</i> <i>I. aurita</i> <i>C. adriatica</i> <i>T. iernis</i> <i>C. intuta</i> <i>B. leydigii</i> <i>rotundus</i> <i>B. calyciflorus</i> <i>S. pectinata</i> <i>E. dilatata</i>	yeast	standard medium	RIC-amount	conglomerate-covered area and average size of conglomerates	light microscopy
Inductor-specific production of Rotimer-Inductor conglomerates (Fig. 2B)	<i>E. dilatata</i>	BSA epoxy Carmine urea cellulose	standard medium	<i>E. dilatata</i>	conglomerate-covered area and average size of conglomerates	light microscopy
Rotimer producing activity (Fig. 3A)	<i>E. dilatata</i>	Carmine	repetitive induction starvation sodium-azide spermidine temperature salt pH rotifer-media trypsin proteinase K collagenase II triton X-100 SDS DMSO EDTA EGTA TPEN etanol metanol glycerol HCl acetic acid	<i>E. dilatata</i>	conglomerate-covered area and average size of conglomerates	light microscopy
Rotimer dissolution measurements (Fig. 3B)	<i>E. dilatata</i>	Carmine	NaOH trypsin proteinase K collagenase II triton X-100 SDS DMSO EDTA EGTA TPEN etanol metanol glycerol HCl acetic acid	RIC-structure	dissolution time and empirical alterations of the original web quality	light microscopy
Spectroscopic characterization of RIC (Fig. 4)	<i>E. dilatata</i>	epoxy Carmine	standard medium	<i>E. dilatata</i>	infrared wavelength	FTIR
Physiologic effects of the examined RIC in vitro (Fig. 5A)	<i>E. dilatata</i>	BSA	standard medium	<i>C. vulgaris yeast</i> <i>SH-SY5Y cells</i>	motility and intracellular esterase activity	light microscopy and fluorescent plate-reader
The role of Rotimer against beta-amyloid 1-42 (A β 42) aggregates (Fig. 5B)	<i>E. dilatata</i> <i>L. bulla</i> <i>C. intuta</i> <i>S. pectinata</i>	yeast	A β 42	<i>E. dilatata</i> <i>L. bulla</i> <i>C. intuta</i> <i>S. pectinata</i>	motility and intracellular esterase activity	light microscopy and fluorescent plate-reader

rotifer-influencing factors (Fig. 3A; with epoxy inductor). Yeast cell skeleton (as a natural particle) was applied as a common inductor in species-specific RIC production measurements (Fig. 2A). The yeast homogenate, aside from using it as an inductor, compiled two-third of the standard nutrient in the case of all species. The rotifer entities, kept in Petri dish, were treated in populations, during the RIC production-related experiments (Fig. 3A), then they were rinsed twice by standard medium. The investigated animals (20 rotifers/wells) were selected and their RIC production was monitored. There were 10 min breaks between the treatment rounds (20 min/case) under repetitive inductions. After each round, the same rotifers were carefully transported by a micropipette into a new well to start the next cycle. These measurements, together with the starvation experiments, were performed under total nutrient depletion, in order to attenuate the biopolymer synthesis in animals. The NaN₃ (20 μ M) and spermidine (50 μ M) treatments were carried out after 100 \times dilutions from stock solutions. During the salt

concentration (0 or 1 g/L) and pH (6 or 8) studies, the final concentrations were provided by transferring the supernatant instead of the dilution. Supplemented composition of standard medium to 1 g/L dose was implemented by adding extra NaHCO₃. Epoxy beads were applied as an inductor in these experiments, because the RPC index (in statistics) of this agent proved to be the best (Suppl. Fig. 1). In order to assess the sublethal dose of NaN₃, the swimming speed (465 \pm 22 μ m/s in normal case) of rotifers was monitored as a viability marker to measure its dose-response to NaN₃ (Suppl. Fig. 2). The detailed general outline of the supplemental experiments is presented by Suppl. Table. Before investigating the inductor-cohesive-stability of Rotimer to reveal the structure of RIC (Fig. 3B; Carmine inductor, except of NaOH, where it was Epoxy), the animals were carefully removed by a micropipette. Then, the well-content was supplemented by the 10 \times concentration of treatment agents (enzymes, solvents, chelators, alcohols and pH-solutions). These RIC-influencing-factors were the followings: normal supernatant media

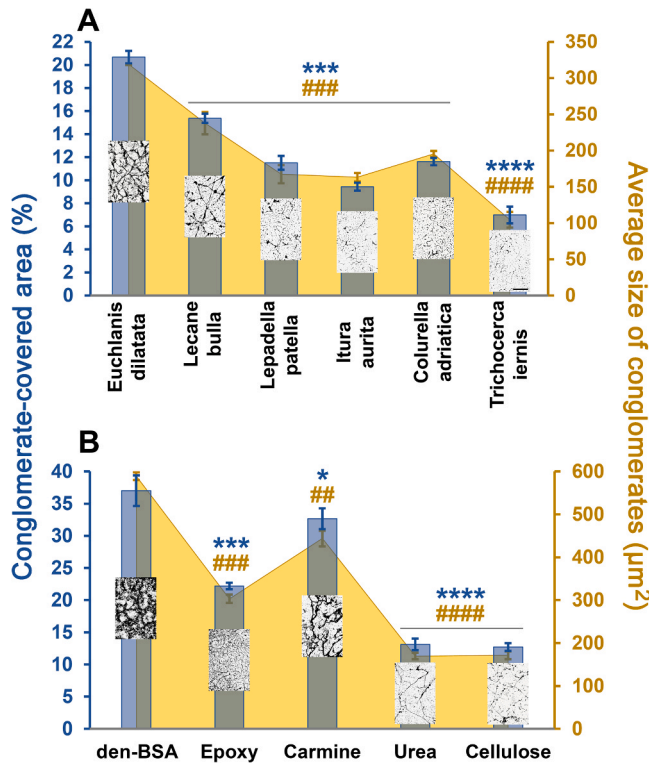


Fig. 2. Rotifer- and inductor-specific production of RIC. Monogonants with different ‘Rotimer-Inductor Conglomerate’ (RIC) producing capacity (A) and the impacts of various inductors on the web structure (B) are presented by the RIC-covered area (%; blue) and the average size of RIC (µm²; yellow). The species-specific webs of RIC are shown by the representative photos on each columns (scale bars: 500 µm). Various Rotimer-inductors were measured on the most productive *E. dilatata* (B), where the representative pictures of the different inductor-specific RIC fibers are presented on the columns (scale bars: 500 µm). The investigated agents were denatured bovine serum albumin (den-BSA), epoxy beads, Carmin, urea and cellulose. The error bars represent S.E.M. One-way ANOVA with Bonferroni post hoc test was used for statistical analysis, the levels of significance are p^{***}### ≤ 0.001 (*, significant difference from *E. dilatata* (A) or from denatured-BSA group (B) in RIC-covered area; # significant difference from *E. dilatata* or from denatured-BSA group (B) in average size of RIC). The black line above the bars means that all these ones show the same level of significance. (For interpretation of the references to colour in this figure legend, the reader is referred to the web version of this article.)

of rotifers, trypsin (1%), Proteinase K (0.5 mg/mL), Collagenase II (3 mg/mL), Triton X-100 (1%), SDS (1%), DMSO (70%), EDTA (0.1 M), EGTA (0.1 M), TPEN (0.1 M), EtOH (70%), MeOH (70%), Glycerol (70%), HCl (1 M), acetic acid (70%) and NaOH (1 M). The concentrations were applied at the highest recommended level by manufacturers. All manipulations were performed slowly and carefully to avoid the fluid flow destroying the RIC web. The disruption of the fiber (mechanical resistance against fluid flow) was measured under the microscope (25× magnification) using the removed and transferred micropipettor (at 45° angle, 3 mm from RIC web) of the micro-plate reader (NOVostar, BMG, Offenburg, Germany). The RIC-stability was provoked by max. 230 µL/s flow velocity (injected volume: 50 µL) where the fibers tore (end of **Suppl. Video**).

Supplementary material related to this article can be found online at [doi:10.1016/j.ecoenv.2020.111666](https://doi.org/10.1016/j.ecoenv.2020.111666).

2.5. The Rotimer and RIC detection with scanning electron microscope

The Rotimer formations (fibers and glues) seemed to be undetectable under inverted light microscope; therefore, analysis with scanning electron microscope (SEM; **Fig. 1L**) was performed. For these series of

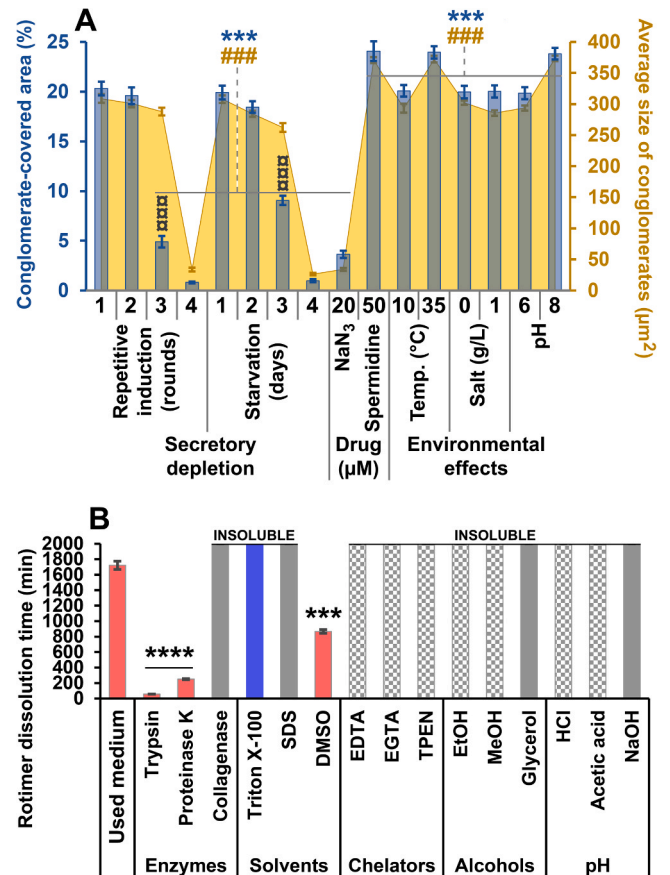


Fig. 3. Rotimer-influencing factors: in vivo secretion and in vitro dissolution. The effects of different conditions on *E. dilatata* Rotimer producing activity (A) were monitored by ‘Rotimer-inductor conglomerate’ (RIC)-covered area (%; blue) and average size of RIC (µm²; yellow). The examined conditions were different secretory depletion methods: repeated induction by carmin (rounds) or induction during starvation (days). The applied drugs were the toxic Na₃ and beneficial spermidine. The investigated environmental conditions were the temperature (4 °C and 30 °C), concentration of salts (0 and 1 g/mL) and various pH (6 and 8). Rotimer dissolution-related experiments were performed by applying various solvents and drug candidate groups (B), which were the following: various used by the rotifers (control); enzymes (trypsin, proteinase K, collagenase II); solvents (triton X-100, SDS, DMSO); chelators (EDTA, EGTA, TPEN); alcohols (EtOH; MeOH, glycerol) and pH-related chemical compounds (HCl, acetic acid, NaOH). The columns represent the dissolution time (min) and their colors show the empirical alterations of the original web quality, where the red stands for dissolution; the blue means the conservation in original high quality; the gray shows the insolubility (during 2000 min) and gray square represents the formation of high RIC aggregates. The error bars show S.E.M. One-way ANOVA with Bonferroni post hoc test was used for statistical analysis; the levels of significance are p^{***}###, α ≤ 0.001 and p^{****} ≤ 0.0001 (*, significant difference between the columns above or below the upper or the lower gray lines (A) in percentage of RIC-covered area or from the standard environment (B); #, significant difference between the columns above or below the upper or the lower gray lines (A) in average size of the conglomerates; α, significant between the percentage of RIC-covered area and percentage of average size of the conglomerates in the relevant conditions). The black line above the bars means that all these ones show the same level of significance. (For interpretation of the references to colour in this figure legend, the reader is referred to the web version of this article.)

experiments, the best and smallest stimulator, epoxy, was used (50 µg/mL) to induce Rotimer secretion and RIC formation in the most productive species, *E. dilatata*. The RIC was produced on a round glass coverslip which was washed with 96% EtOH, DW and finally with standard medium before being experimented in 24-well plates (one coverslip/well/30 mature rotifer). The animals produced RIC for 30 min

on the coverslip under standard conditions, then, they were carefully removed by a micropipette. The glass surface covered by RIC was checked under light microscope, then, it was let dry at room temperature for 1 h. The samples were coated with gold. The selected areas (based on their quality) were subjected to SEM (Zeiss EVO MA 10, Carl Zeiss, Oberkochen, Germany). The sample-carrier coverslip was fixed onto a stub using a double-sided carbon tape. The samples were coated with gold using a Quorum Q150R sputter coater during 120 s. The fine structure of the RIC was observed and photo-documented with the SEM at different magnifications (from 846X to 40.47KX). The detections were operating at 10 kV with an 8-mm working distance, using a secondary electron detector in high vacuum mode. The white balance of SEM photographs was normalized.

2.6. Analysis of Rotimer containing RIC with FTIR spectroscopy

In order to perform FTIR spectroscopy (Kowalczyk and Pitucha, 2019) measurements, Rotimer containing RIC samples were prepared. As a first step, *E. dilatata* ($n = 500 \pm 30$ individuals) populations were harvested into Petri dishes (55 cm² area). Then, the inductor (Carmine) was added to the rotifer-containing standard medium for 20 min. The produced RIC was mechanically homogenized by a pipette. The animals were removed by filtration using a plastic web (pore size 50 μ m). The animal-free, but RIC-containing solution was then centrifuged by 4000 \times g for 20 min (in 14 mL volume centrifuge tubes) at room temperature. The supernatant was decanted and the pellet was used for FTIR measurements.

The concentrated RIC solution (15 μ L) was dropped onto the surface of potassium bromide pastilles (200 mg, 13 mm diameter) three times, which were compressed with hydraulic press (Specac Inc., UK). The pastilles were then desiccated for 48 h in silica gel filled desiccator. The FTIR spectra of various samples were measured with a Thermo Nicolet Avatar 330 FTIR spectrometer (Thermo Fisher Scientific Ltd., Waltham, MA, USA) using a Transmission E. S. P. accessory applying 128 scans at a resolution of 4 nm. Data were collected with EZ OMNIC software, while spectrum analysis was performed with Spectragryph 1.2.13 (Friedrich Menges, Oberstdorf, Germany) software. A strong shift of baseline was observed due to the beam scattering on the undissolved or recrystallized carmine particles. Furthermore, due to the low signal intensities, resulted by the low sample concentrations, the presence of negative peaks was observed in the 2800–3000 cm⁻¹ CH stretching region. It was also resulted by the uncompensated background signal of hydrophobic protective coating on the optical elements of the spectrometer. These artificial distortions and the uncompensated CO₂ signals in the region of 2280–2390 cm⁻¹ were cut off from the spectrum prior to baseline correction. To compensate the effect of beam scattering two step baseline correction, simple linear correction, followed by a secondary adaptive correction (coarseness = 10) was applied prior to the analysis.

2.7. Bioactivity-related viability assays

In all viability-related experiments (Table 1), based on Calcein-AM (stock solution: 1 mg/mL in DMSO; final concentration was 5 μ M), the labeling interval was 1 h at room temperature in the dark. The viability (cell-fluorescence) and motility (movement of cells) of algae and yeast cells (Fig. 5A) were measured in separate 24-well plates. Confluent cell population (120 ± 11 cells/well) was applied in cytoplasmic calcium detection where the fluorescence intensity (FI) of intracellularly trapped Calcein (ex. 490, em. 520; calibration/gain adjustment was 1% of the maximal relative intensity) was detected. Separate cells (4–5 cells/well) were administered in motility-related investigations. After 24 h treatment with RIC (used inductor: den-BSA) and its reference controls (untreated or only den-BSA treated), the FI of intracellular calcium-specific dye and the moving action in different setups were measured, in the latter case the detection interval of cell motility was 10 min (unit: μ m/min).

To test the physiologic effects of the examined RIC (containing Rotimer) in vitro, we applied the SH-SY5Y neuroblastoma cells. The viability (fluorescence) and motility (cell migration) of SH-SY5Y cells were separately measured in 96-well plates. The FI of intracellular Calcein was detected after 24 h treatment with den-BSA or its RIC in a cell culture with confluent monolayer (cell number was 110 ± 8 in one well). Detection interval in cell motility assay (4–5 cells/well) took for 6 h (unit: μ m/h) after one-day-treatment.

The potential role of Rotimer against A β 42 aggregates was investigated in four different species (Fig. 5B; *E. dilatata*; *L. bulla*; *C. intuta*; *S. pectinata*). Concentration of A β 42 stock solution was 1 mg/mL (DW) with 3 h (25 °C, pH 3.5) aggregation period. Neutralization (to pH 7.5) of this solution was performed with NaOH (1 N). After 10-fold dilution with standard medium, the final (working) concentrations were 100 μ g/mL. After harvesting, 30 ± 2 mature rotifers per well ($n = 24$ well/species in 96 well-plate) were treated in 0.2 mL volume. The treatment period was 5 days in standard conditions (24 °C; 40% air humidity; standard media). The depletion protocol was performed before the A β 42 was administered and this protocol was in line with the one applied in Fig. 3A-treatment. Every A β 42-treated group had its own untreated control, which was the reference (100%) in every case. Two parameters of viability were measured, namely the number of rotifers alive and the intracellular esterase activity (indicated by relative fluorescence intensity of Calcein-AM). The populations were observed under light microscope (63X) combined with digital camera (Nikon D5100). The protocol of Calcein-AM measurements were the same with the one applied in Fig. 5A.

2.8. Statistics

The error bars represent the standard error of the mean (S.E.M.). For comparative statistical analysis, the one-way ANOVA was used followed by the Bonferroni post hoc test with SPSS 23.0 (SPSS Inc, Chicago, IL, USA) software for Windows. The homogeneity and normality of the data were checked, and they were found suitable for ANOVA followed by Bonferroni post hoc test. The RPC index (RPC_i) is a relative unit, which was calculated by the following formula: $RPC_i = ASC/ASIP * CA/NR$; ASC: Average Size of Conglomerates (μ m²); ASIP: Average Size of Inductor Particles (μ m²); CA: Covered Area (%); NR: Number of Rotifers. The different levels of significance are indicated as follows: p^{*}, # ≤ 0.05 , p^{**}, $\square \leq 0.01$, p^{***}, ##, $\square \square \leq 0.001$ and p^{****} ≤ 0.0001 (all marks are defined in the given figure legend).

3. Results and discussion

In academic literature, no one has yet described filamentous biopolymer secretion in rotifers, nor in monogonants. The aim of the present study was to describe and characterize a novel rotifer-specific biopolymer, called 'Rotimer' in monogonant rotifers. Biopolymers are scientific hotspots for which researchers have been recently gaining more academic interest (Humenik et al., 2019).

The above mentioned rotifer-specific fiber production was observed in six (Fig. A-F) different freshwater monogonants, which were the followings: *E. dilatata*, *L. bulla*, *L. patella*, *I. aurita*, *C. adriatica* and *T. iernis*. All investigated animals can be frequently found in lakes or other natural waters; furthermore, they are well-established model organisms of ecotoxicological (Walsh et al., 2009; Suthers et al., 2019;) and pharmaceutical researches (Gutierrez et al., 2020). After permanent laboratory culturing the *E. dilatata* and *L. bulla* proved to have the most intensive RIC production capacity (RPC) out of the six investigated species. Representative photo (Fig. 1K) about RIC formation produced by *E. dilatata* was taken.

Nevertheless, we observed RIC formations in the original medium of wild-type animals collected from their natural habitat, meaning they are able to produce Rotimer in nature. Since, the secreted Rotimer alone could not experientially be detected by light microscope; therefore, its

existence could only be proved with particle adhesion.

No refractions of the Rotimer were detected between two inductor particles at 1000X magnification. In order to try to optically visualize this biopolymer, different types of dyes (Trypan blue, Light green SF, Orange G, Neutral red, Methylene blue, Acridine orange, Ponceau S, Bromophenol blue, Congo red, Fuchsin, Coomassie brilliant blue G-250 or R-250, Luxol fast blue and Methyl red) were tested, diluted in DW or EtOH, but no success was gained in labeling them. Fibers drawn by *E. dilatata* monogonants are very thin (33 ± 3 nm cross section) and they can only be observed by SEM. The produced exogenic Rotimer (Fig. 1L) can either be filamentous (arrow) or glue-like (dashed arrow). Both biopolymer forms are secreted parallelly and attach to the surface of inductors. Secretion of Rotimer could be mechanically induced by approximately 2.5–50 μm diameter particles, respectively in *E. dilatata*. No RIC production above or under this range was observed. Beyond size-specificity, the Rotimer induction does not depend on the qualitative properties (e.g. type of material) of inductors. Percentage of conglomerate-covered area exponentially increased with time, characterizing the kinetics of RIC production in *E. dilatata* (Fig. 1M). The saturation of confluent covering in the measured area took 18–20 min in standard medium. Contrary to monogonants, no fiber-like formations were detected in the case of bdelloids; however, the attachment of their eggs and coating with nutrient particles on the bottom of the flask were observed. Based on these empirical data, bdelloids may likely produce polymer-type secretions. The presence and existence of Rotimer is optically indicated by RIC formation that is fibrous, viscoelastic, floating in fluid (3D formation) and breakable by water jet (Suppl. Video; visible at the 56–59 s). Rotifers are able to find the web-formation from a relatively high distance in their dimensions by directional approaching; therefore, it is assumed that the fiber has a specific surface, which can be recognized by them. The longest detected fiber was 1.3 mm (floating in water between two attached ends).

Rotimer was secreted by six different rotifers (Fig. 2A) and this product was investigated to assess which species could be the most effective producers under yeast induction. The representative photos of RIC present which type of rotifers produce it by creating different web structures. Various sizes of Rotimer-inductors were tested on *C. intuta*, *B. leydigii rotundus*, *B. calyciflorus* and *S. pectinata*; however, no structured fiber-like polymer production was found. In the quantitative characterization of RIC, the percentage of covered area and the average size of conglomerates were monitored. The *E. dilatata* significantly showed the highest measures in both parameters, thus, this species seemed to be the best producer of RIC formation. The next step was to find out whether there were other non-toxic inductors which might have been more effective than yeast (Fig. 2B). The potential candidates were tested and the average particle size (μm^2 ; excluding the adhesive Rotimer) were also determined: den-BSA, 165 ± 22 ; epoxy, 7.5 ± 0.5 ; Carmine, 50 ± 14 ; urea, 83 ± 21 ; cellulose, 75 ± 18 as opposed to the reference yeast, 45 ± 3 .

All investigated inductor-types were able to induce Rotimer-secretion, manifested by RIC, that are showed by the representative photos. Accordingly, the process of induction is not specific, but it is exclusively triggered by the size of particles. The RIC composed den-BSA-Rotimer web showed the highest value in the conglomerate-covered area and in the average size of conglomerates. The epoxy and Carmine were also applicable in further experiments. The urea and cellulose were able to induce RIC production; however, their efficiency were much lower than that of the other inductors.

The size-related parameters of particles presented the differences between them, but they were not enough to provide a comprehensive characterization. In order to overcome this problem, the RPC index was developed. This quantified relative index becomes higher, when there are fewer animals the inductor particle size is low and the formed conglomerates are large. According to the RPC index (RPC_i), the epoxy was the most effective inductor, the second one was Carmine and the third one was den-BSA (Suppl. Fig. 1). The most adequate type of inductor was

chosen, considering its chemical and biological properties, and RPC_i in the relevant experiments. Based on the universal adhesive property of Rotimer, it may prove to be a useful tool in waste water cleaning. Similarly to other biopolymers (Kalia and Avérous, 2011), it may have a potential industrial use.

As the RIC web seemed to be a very complex formation and it is characteristic to some monogonants, we wanted to test how the different environmental factors influence its production (Fig. 3A). The yeast was applied as an inductor, since it is also a component of the food of rotifers. After repetitive inductions, the depletion of the Rotimer-resources was observed in *E. dilatata*. After the third round of induced stimulation, the average size of conglomerates did not alter, nonetheless, the percentage of conglomerate-covered area significantly decreased. Differences between both of the measured parameters were found in the first-second rounds and third-fourth rounds. Presumably, the animals ran out of the materials needed for secretion and there was probably not enough time for resynthesis. It is supposed that active synthesis of Rotimer is required for RIC production which might be an energetically active process.

After starvation, we observed a second mode of depletion of Rotimer secretion due to the lack of nutrients (Fig. 3A). The size of conglomerates remained the same, after three days without food, but the covered area was significantly reduced. Remarkable alterations of monitored parameters were seen between RIC productions after the first-second day and third-fourth day of starvation. As there was no food available, the rotifers probably used the endogenous Rotimer substrate as energy deposit. The regeneration time of RIC production was 30 ± 4 min applying yeast homogenate or 140 ± 11 min applying den-BSA as inductors as well as foods in starvation-depleted *E. dilatata* entities. In the presence of epoxy, Carmine, urea and cellulose there was no RIC production for more than 6 h incubation time in depleted animals. The systemic production of Rotimer in rotifers is relatively quick and is highly nutrient-dependent.

To measure the properties of the viability marker of Rotimer secretion, the highest sublethal dose of NaN_3 (Suppl. Fig. 2) in *E. dilatata* was determined, which had no toxic effect on them for 6 h. The NaN_3 was applied with the purpose of revealing how the partial mitochondrial dysfunction may influence Rotimer secretion. Based on the current literature, we used the swimming speed as an adequate reference viability marker of monogonants (Dahms et al., 2011; Chen et al., 2014; Guo et al., 2012; Dong et al., 2020). The swimming speed of control animals was 465 ± 22 $\mu\text{m}/\text{s}$ in the setup and the RIC production was also manifested by this kind of speed. Deceleration in swimming speed at doses between 50 and 500 μM was observed and thereby, 20 μM was selected for the next experiment. The applied dose of sodium azide had a negative effect on biopolymer formation, presenting the sublethal viability marker properties of Rotimer secretion. This inhibitor of terminal oxidation significantly and parallelly decreased both the percentage of conglomerate-covered area and the average size of conglomerates. Based on previous results, NaN_3 is a mitochondrial toxin, which reduces the energy synthesis by lowering the efficacy of mitochondrial respiration (Olah et al., 2017). In contrast with that, spermidine had positive effects on all parameters. This is in line with our previous publications where the calorie-mimetic spermidine showed beneficial impact on mitochondrial function and physiology (Datki et al., 2019). These data also supported the assumption that RIC production requires energy. Surprisingly, the lower temperature (10 °C) did not decrease the monitored parameters compared to its controls, while the higher temperature (35 °C) was able to stimulate production. Results found were in line with the publication of Li et al. (2019), who measured different life parameters (trade-offs between egg size and egg number, current reproduction and future survival) of *E. dilatata* at 14 °C, 20 °C and 26 °C. By increasing temperature, the lifespan, pre-mature- and reproductive periods decreased; however, the rate of population growth elevated. Similarly to RIC production, warmer temperature was beneficial for monogonants. Directly using *E. dilatata* entities after isolation,

the elevation (1 g/L) or the reduction (DW) of salt concentration had no effect on RIC production compared to the standard medium (Fig. 3A); however, when these animals were left to rest (washed) in completely ion-free medium for half an hour, the RPC disappeared. The salinization of coastal freshwater raises serious concerns on the protection of their ecosystems (Venâncio et al., 2018). High salinity induces oxidative stress, having a negative impact on lipid metabolism in another monogonant rotifer, *Brachionus koreanus*, demonstrated by Lee et al. (2018). Contrary to these comprehensive data about the salt-sensitivity of monogonants, it was observed that the extreme osmolarity had no negative impact on the monitored parameters. Lower pH (6) did not reduce the above mentioned parameters, while the higher pH (8) was beneficial for RIC production. The pH 6 represented the lower pH range of most natural waters found in the United States and across Europe (Cardwell et al., 2018), where monogonants are found, such as *Brachionus* species which were cultured at different ranges of pH from 6 to 10. The maximum population densities were reached at pH 8. (Gopal et al., 2014).

Furthermore, we were curious to find out how RIC could maintain its integrity in the presence of various chemical agents (Fig. 3B). The structure-preserving stability of particles, adhered by Rotimer, was detected. Although the epoxy seemed to be the best inductor, it could not be applied together with enzymes or ionic molecules due to its superficial specific charges, which may inactivate the applied agents. Carmine was used as inductor in all cases of current experiments, except in the presence of NaOH, because it dissolved these crystals; thus epoxy was added. It was highlighted that RIC lost its integrity in the presence of two-day-old rotifer culture medium, trypsin, proteinase K or DMSO during the time of measurement, suggesting that a protein-type material may fully or partially compose the Rotimer. The RIC preserved its original integrity together with collagenase II, Triton X-100, SDS, glycerol or NaOH. Triton X-100, the nonpolar detergent, showed the highest level of conservation. Moreover, the RIC was extremely aggregated by EDTA, EGTA, TPEN, EtOH, MeOH, HCl or acetic acid without solubilization. It may occur that metal ions and hydration may be necessary for maintaining normal integrity of the Rotimer. Unfortunately, it is very difficult to investigate the Rotimer structure and its components, because right now, we cannot clearly isolate this biopolymer from the relevant inductor. Investigation of this exudate was carried out in the presence of Carmine, a non-proteinous RIC-inductor, with FTIR (Fig. 4).

The FTIR spectrum of the standard medium contains several broad peaks which may be associated with the HCO_3^- and silicic acid content. The spectrum of the Carmine, as inductor molecule, contains two individual peaks in OH stretching region (3732 and 3299 cm^{-1}) belonging to the non-associated and associated OH groups, respectively. The strong right shift of the non-associated peak to 3438 cm^{-1} in the RIC indicates

that Rotimer connects to the inductor molecules via the formation of H-bonds of those OH groups which take no part in intramolecular associations. The appearance of a new peak 3250 cm^{-1} could be connected to the N-H stretching of amine groups of the biopolymer. The peaks associated with the C=O stretching appeared in slightly lower wavenumbers than usually. The C=O stretching of aromatic carboxylic acid is visible at 1645 cm^{-1} , while the peak related to the diaromatic keto groups appeared at 1569 cm^{-1} . The relatively unchanged position of these peaks indicates that these groups are not involved in the formation of RIC, possibly due to their partition in intramolecular associations. The appearance of the new peak at the position of 1612 cm^{-1} is related to the amide II vibrations of the Rotimer backbone. The peaks at 1471 cm^{-1} and 1413 cm^{-1} belong to βOH vibrations of carboxylic and phenolic OH groups respectively, while the peak doublet at 1292 cm^{-1} and 1257 cm^{-1} may be associated with the βOH vibration of secondary alcoholic groups. The peak quadruplet in the $980\text{--}1080\text{ cm}^{-1}$ region belongs to the C-O stretching of various molecular parts. Considerable differences of the pure carmine and carmine-Rotimer complex may be observed in this region, but due to the low signal intensity and strong overlapping peaks the cause of the change may not be clearly identified.

The results of FTIR analysis indicate strong H-bond-based interactions between the inductor Carmine crystals and the Rotimer, which exhibits peptide like nature. However, the separation of Rotimer peaks was impossible due to the strong overlapping of the Carmine and Rotimer signals. The clear molecular identification of the Rotimer structure will require further investigations.

Finally, the intention was to demonstrate the representative bioactivity of monogonants-secreted Rotimer. The physiological effects (viability and motility) of *E. dilatata*-derived RIC with Rotimer content on three different cell types (Fig. 5A) were investigated. Den-BSA was applied as inductor, which can be found in standard medium of human cell culturing; therefore, it had no extra physiologic impact on the cells in the setup. The average movement of cells were properly measurable (algae: $87 \pm 18\ \mu\text{m}/\text{min}$; yeast: $150 \pm 39\ \mu\text{m}/\text{min}$; neuroblastoma: $64 \pm 19\ \mu\text{m}/\text{h}$) in untreated controls. Passive (diffusion-based floating) and active (cell-movement) motility can occur in algae and yeast, while only an active one was detectable in the human neuroblastoma line. The RIC slightly decreased the viability of algae or neuroblastoma, where the toxicity did not reach the LD50; furthermore, it ceased their motility in all types of cells. Based on our previous work (Datki et al., 2018), we were interested in A β -related toxicity in the presence of Rotimer (Fig. 5B). The natural nutrient of rotifers includes aggregated and conglomerated organic masses in their native habitat. Investigation of the harmful A β 2 on rotifers is an interdisciplinary approach in toxicology-related life sciences. Four species were treated with A β 2 aggregates; only two of them secreted Rotimer (*E. dilatata*; *L. bulla*). In

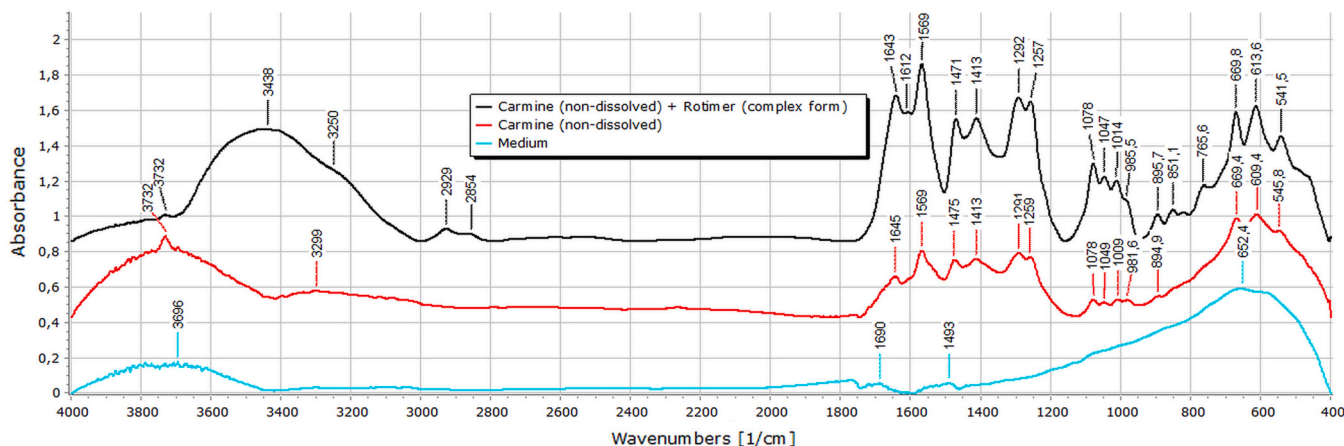


Fig. 4. FTIR spectra of the medium (blue), the Carmine crystals (red) and the Carmine-Rotimer complexes (black). (For interpretation of the references to colour in this figure legend, the reader is referred to the web version of this article.)

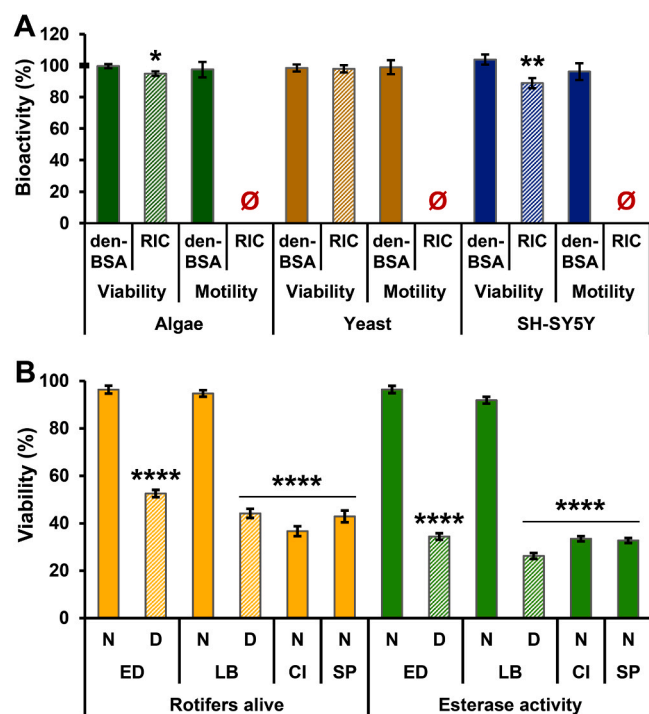


Fig. 5. Bioactivities of monogonant-secreted Rotimer. The special effect of *E. dilatata*-secreted RIC on different types of cell viability and motility (A) is presented. The percentage of bioactivity on viability and motility of algae (*Chlorella vulgaris*; green), yeast (*Saccharomyces cerevisiae*; yellow) and human neuroblastoma cells (SH-SY5Y; blue) was monitored in the presence of untreated control (100%) and denatured bovine serum albumin (den-BSA; full columns; reference control) or 'Rotimer-inductor conglomerate' (RIC; striped columns). The untreated control was 100% marked with bold line on the y-axis. The error bars represent S.E.M. One-way ANOVA with Bonferroni post hoc test was used for statistical analysis; the levels of significance are $p^* \leq 0.05$ and $p^{**} \leq 0.01$ (*, significant difference from untreated control group). The impacts of monogonant-secreted Rotimer on viability in beta-amyloid 1–42 (A β 42)-treated populations (B) are shown. Four species were investigated: *Euchlanis dilatata* (ED); *Lecane bulla* (LB); *Cephalodella inuata* (CI) and *Synchaeta pectinata* (SP). The number of rotifers alive (orange) and the relative fluorescence intensity of esterase activity (green) were measured and their percentages are presented. The species-specific untreated control was the reference 100% (data not shown). The full columns represent the A β 42-treated normal (N) populations, while the striped ones indicate the A β 42-administered and Rotimer-depleted (D) ones. The error bars represent S.E.M. One-way ANOVA with Bonferroni post hoc test was used for statistical analysis; the level of significance is $p^{****} \leq 0.0001$ (*, significant difference from untreated species-specific control group). The black line above the bars means of treatments with the same level of significance. (For interpretation of the references to colour in this figure legend, the reader is referred to the web version of this article.)

secretion capable animals the Rotimer depletion was applied to investigate the role of this biopolymer in A β -sensitivity/toxicity. It was found that *E. dilatata* and *L. bulla* are not sensitive to A β 42 aggregates in their normal state, where the number of rotifers alive and esterase activity was the same as in the case of species-specific untreated controls (100%). After in vivo biopolymer-depletion the animals lost their resistance against neurotoxic aggregates; and the measured parameters were significantly reduced, compared to their controls. The same phenomenon (significant decrease) was observed in those animals (*C. intuta*; *S. pectinata*), which did not secrete exogenic filamentous biopolymer. The number of rotifers alive refers to the in vivo characteristics of the investigated populations, while the esterase activity indicates the cellular membrane integrity of the individuals. These results suggest that Rotimer can play an essential protective role against A β aggregate-toxicity in some monogonant rotifers. Although the molecular

structure and the holistic biological/biotechnological significance of this proteinous-nature polymer is yet unknown, it will need further physical-chemical analysis.

4. Conclusion

The current study presents a novel and bioactive rotifer-specific biopolymer (having filamentous and glue-like forms), called Rotimer, derived from certain monogonants. In the presence of this exudate, its motility-inhibition effects in different cell types and its protective impacts in rotifers against neurotoxic aggregates were observed. This viscoelastic and chemically fairly resistant product might be a promising active molecule and drug candidate for ecotoxicological protection (e.g. water-clearing) or in researches related to cancer- and neurodegenerative diseases. The specific molecular structure and the holistic biological/biotechnological significance of this proteinous natural polymer is yet unknown.

Funding

The authors received no specific funding for this work.

Supplementary text

Methods

The empirical presentation of Rotimer secretion and RIC production can be seen in the video (**Suppl. Video**; MOV, full HD resolution, 16:9 ratio, 30 frame/s). The RIC producing capacity index (RPC_i) was calculated by the formula described in the statistics (**Suppl. Fig. 1**). The doses of Na₃N were applied in 100x dilutions (**Suppl. Fig. 2**).

CRediT authorship contribution statement

Conceptualization, Zs.D. and Z.G.O.; Methodology, Zs.D., Z.G.O., E. A., E.B., T.S. and I.Cs.; Validation, Zs.D., Z.G.O., and K.Zs.; Formal analysis, Zs.D., Z.G.O. and E.B.; Investigation, Zs.D., Z.G.O., E.B., E.A. and T.S.; Resources, Zs.D., J.K.; Data curation, Zs.D., Z.G.O., E.A. and T. S.; Writing-original draft preparation, Zs.D. and Z.G.O.; Writing-review and editing, Zs.D., Z.G.O., E.B. and J.K.; Visualization, Zs.D.; Supervision, Zs.D., Z.G.O., I.Cs. and J.K.; Project administration, Zs.D., Z.G.O.; Funding acquisition, Zs.D. and J.K.

Acknowledgments

The authors wish to thank to Anna Szentgyorgyi MA, a professional in English Foreign Language Teaching for proofreading the manuscript.

Conflicts of interest

No conflicts of interests declared.

Appendix A. Supporting information

Supplementary data associated with this article can be found in the online version at [doi:10.1016/j.ecoenv.2020.111666](https://doi.org/10.1016/j.ecoenv.2020.111666).

References

- Cardwell, A.S., Adams, W.J., Gensemer, R.W., Nordheim, E., Santore, R.C., Ryan, A.C., Stubblefield, W.A., 2018. Chronic toxicity of aluminum, at a pH of 6, to freshwater organisms: empirical data for the development of international regulatory standards/criteria. *Environ. Toxicol. Chem.* 37, 36–48. <https://doi.org/10.1002/etc.3901>.
- Chandra, R., Rustgi, R., 1998. Biodegradable polymers. *Prog. Polym. Sci.* 23, 1273–1335.
- Chen, Q., Peng, D., 2019. Nematode chitin and application. *Adv. Exp. Med. Biol.* 11421, 209–219. https://doi.org/10.1007/978-981-13-7318-3_10.

- Chen, J., Wang, Z., Li, G., Guo, R., 2014. The swimming speed alteration of two freshwater rotifers *Brachionus calyciflorus* and *Asplanchna brightwelli* under dimethoate stress. *Chemosphere* 95, 256–260. <https://doi.org/10.1016/j.chemosphere.2013.08.086>.
- Dahms, H.U., Hagiwara, A., Lee, J.S., 2011. Ecotoxicology, ecophysiology, and mechanistic studies with rotifers. *Aquat. Toxicol.* 101, 1–12. <https://doi.org/10.1016/j.aquatox.2010.09.006>.
- Datki, Z., Galik-Olah, Z., Bohar, Z., Zadori, D., Fulop, F., Szatmari, I., Galik, B., Kalman, J., Vecsei, L., 2019. Kynurenic acid and its analogs are beneficial physiologic attenuators in bdelloid rotifers. *Molecules* 24, 2171. <https://doi.org/10.3390/molecules24112171>.
- Datki, Z., Juhász, A., Gálfi, M., Soós, K., Papp, R., Zádori, D., Penke, B., 2003. Method for measuring neurotoxicity of aggregating polypeptides with the MTT assay on differentiated neuroblastoma cells. *Brain Res. Bull.* 62, 223–229. <https://doi.org/10.1016/j.brainresbull.2003.09.011>.
- Datki, Z., Olah, Z., Hortobagyi, T., Macsai, L., Zsuga, K., Fulop, L., Bozso, Z., Galik, B., Acs, E., Foldi, A., Szarvas, A., Kalman, J., 2018. Exceptional in vivo catabolism of neurodegeneration-related aggregates. *Acta Neuropathol. Commun.* 6, 6. <https://doi.org/10.1186/s40478-018-0507-3>.
- Debortoli, N., Li, X., Eyres, I., Fontaneto, D., Hespels, B., Tang, C.Q., Flot, J.F., Van Doninck, K., 2016. Genetic exchange among bdelloid rotifers is more likely due to horizontal gene transfer than to meiotic sex. *Curr. Biol.* 26, 723–732. <https://doi.org/10.1016/j.cub.2016.01.031>.
- Dong, L.L., Wang, H.X., Ding, T., Li, W., Zhang, G., 2020. Effects of TiO₂ nanoparticles on the life-table parameters, antioxidant indices, and swimming speed of the freshwater rotifer *Brachionus calyciflorus*. *J. Exp. Zool. Ecol. Integr. Physiol.* 333, 230–239. <https://doi.org/10.1002/jez.2343>.
- Ehrlich, H., 2019. *Marine Biological Materials of Invertebrate Origin*. Springer International Publishing AG. <https://doi.org/10.1007/978-3-319-92483-0> part of Springer Nature 2019.
- Fontaneto, D., Westberg, M., Hortal, J., 2011. Evidence of weak habitat specialisation in microscopic animals. *PLoS One* 6, e23969. <https://doi.org/10.1371/journal.pone.0023969>.
- Ganesana, A.R., Guru, M.S., Balasubramanian, B., Mohan, K., Liu, W.C., Arasu, M.V., Al-Dhabi, N.A., Durairamian, V., Ignacimuthu, S., Sudhakar, M.P., Seedeve, P., 2020. Biopolymer from edible marine invertebrates: a potential functional food. *J. King Saud. Univ. Sci.* 32, 1772–1777. <https://doi.org/10.1016/j.jksus.2020.01.015>.
- Gopal, P., Citarasu, T., Punitha, S.M.J., Selvaraj, T., Albindas, S., Sindhu, A.S., Babu, M. M., 2014. Influence of physical and nutritive parameters on population and size variation in two species of rotifers. *J. Aqua Trop.* 29, 121–134.
- Guo, R., Ren, X., Ren, H., 2012. A new method for analysis of the toxicity of organophosphorus pesticide, dimethoate on rotifer based on response surface methodology. *J. Hazard. Mater.* 237, 270–276. <https://doi.org/10.1016/j.jhazmat.2012.08.041>.
- Gutierrez, M.F., Molina, F.R., Frau, D., Mayora, G., Battauz, Y., 2020. Interactive effects of fish predation and sublethal insecticide concentrations on freshwater zooplankton communities. *Ecotoxicol. Environ. Saf.* 196, 110497. <https://doi.org/10.1016/j.ecoenv.2020.110497>.
- Hassan, M.E., Bai, J., Dou, D.Q., 2019. Biopolymers; definition, classification and applications. *Egypt. J. Chem.* 62, 1725–1737. <https://doi.org/10.21608/EJCHEM.2019.6967.1580>.
- Hennebert, E., Gregorowicz, E., Flammang, P., 2018. Involvement of sulfated biopolymers in adhesive secretions produced by marine invertebrates. *Biol. Open* 7, bio037358. <https://doi.org/10.1242/bio.037358>.
- Humenik, M., Pawar, K., Scheibel, T., 2019. Nanostructured, self-assembled spider silk materials for biomedical applications. *Adv. Exp. Med. Biol.* 1174, 187–221. https://doi.org/10.1007/978-981-13-9791-2_6.
- Kalia, S., Avérous, L., 2011. *Biopolymers: Biomedical and Environmental Applications*, First ed. John Wiley and Sons Inc, Hoboken, New Jersey.
- Kamiya, H., Sakai, R., Jimbo, M., 2006. Bioactive molecules from sea hares. *Prog. Mol. Subcell. Biol.* 43, 215–239. https://doi.org/10.1007/978-3-540-30880-5_10.
- Kertész, K., 1894. *Budapest és környékének Rotatoria-Faunája*. Rózsa Kálmán és Neje Print, Budapest.
- Kisugi, J., Kamiya, H., Yamazaki, M., 1992. Biopolymers from marine invertebrates. XII. A novel cytolytic factor from a hermit crab, *Clibanarius longitarsus*. *Chem. Pharm. Bull.* 40, 1641–1643. <https://doi.org/10.1248/cpb.40.1641>.
- Koste, W., 1978. *Rotatoria - Die Radertiere Mitteleuropas*. Ein Bestimmungswerk, begründet von Max Voigt. Überornung Monogononta, Berlin - Stuttgart, pp. 285–289. <https://doi.org/10.1002/iroh.19800650226>.
- Kowalczyk, Dorota, Pitucha, Monika, 2019. Application of FTIR method for the assessment of immobilization of active substances in the matrix of biomedical materials. *Materials* 12, 2972. <https://doi.org/10.3390/ma12182972>.
- Kutikova, L.A., 1970. Kolovratki fauna SSSR. Fauna SSSR, vol. 4. Akademia Nauk Leningrad, pp. 362–367.
- Lee, M.C., Park, J.C., Yoon, D.S., Han, J., Kang, S., Kamizono, S., Om, A.S., Shin, K.H., Hagiwara, A., Lee, J.S., 2018. Aging extension and modifications of lipid metabolism in the monogonont rotifer *Brachionus koreanus* under chronic caloric restriction. *Sci. Rep.* 8, 1741. <https://doi.org/10.1038/s41598-018-20108-7>.
- Li, W., Lian, B., Niu, C., 2019. Effects of temperature on life history strategy of the rotifer *Euchlanis dilatata*. *Zool. Sci.* 36, 52–57. <https://doi.org/10.2108/zs170096>.
- Macasai, L., Olah, Z., Bush, A.I., Galik, B., Onody, R., Kalman, J., Datki, Z., 2019. Redox modulating factors affect longevity regulation in rotifers. *J. Gerontol. Biol. Sci. Med. Sci.* 74, 811–814. <https://doi.org/10.1093/geronol/gly193>.
- Mohamed, S., El-Sakhawy, M., El-Sakhawy, M.A., 2020. Polysaccharides, protein and lipid -based natural edible films in food packaging: a review. *Carbohydr. Polym.* 238, 116178. <https://doi.org/10.1016/j.carbpol.2020.116178>.
- Muhlia-Almazán, A., Sánchez-Paz, A., García-Carreño, F.L., 2008. Invertebrate trypsin: a review. *J. Comp. Physiol. B* 178, 655–672. <https://doi.org/10.1007/s00360-008-0263-y>.
- Nogrady, T., Segers, H., 2002. *Rotifera Vol. 6: Asplanchnidae, Gastrotrichidae, Liniidae, Microtrichidae, Synchaetidae, Trocosphaeridae and Filinia*. In: Dumont, H.J. (Ed.), *Guides to the Identification of the Microinvertebrates of the Continental Waters of the World*. Leiden, pp. 59–79.
- Olah, Z., Bush, A.I., Aleksza, D., Galik, B., Ivitz, E., Macasai, L., Janka, Z., Karman, Z., Kalman, J., Datki, Z., 2017. Novel in vivo experimental viability assays with high sensitivity and throughput capacity using a bdelloid rotifer. *Ecotoxicol. Environ. Saf.* 144, 115–122. <https://doi.org/10.1016/j.ecoenv.2017.06.005>.
- Olatunji, O., 2020. *Aquatic Biopolymers, Understanding their Industrial Significance and Environmental Implications*. Springer International Publishing. <https://doi.org/10.1007/978-3-030-34709-3>.
- Pallas, P.S., 1766. *Elenchus zoophytorum systems generum adumbrations generaliores et specierum cognitarum succinactas descriptions cum selectis auctorum synonymis*. Hagae Comitum 451pp.
- Rahman, M.A., 2019. Collagen of extracellular matrix from marine invertebrates and its medical applications. *Mar. Drugs* 17, 118. <https://doi.org/10.3390/md17020118>.
- Robeson, M.S., King, A.J., Freeman, K.R., Birky Jr., C.W., Martin, A.P., Schmidt, S.K., 2011. Soil rotifer communities are extremely diverse globally but spatially autocorrelated locally. *Proc. Natl. Acad. Sci. USA* 108, 4406–4410. <https://doi.org/10.1073/pnas.1012678108>.
- Ruiz-Torres, V., Rodríguez-Pérez, C., Herranz-López, M., Martín-García, B., Gómez-Caravaca, A.M., Arráez-Román, D., Segura-Carretero, A., Barrajón-Catalán, E., Micol, V., 2019. Marine invertebrate extracts induce colon cancer cell death via ROS-mediated DNA oxidative damage and mitochondrial impairment. *Biomolecules* 9, 771. <https://doi.org/10.3390/biom9120771>.
- Snell, T.W., Johnston, R.K., Gribble, K.E., Mark Welch, D.B., 2015. Rotifers as experimental tools for investigating aging. *Invertebr. Reprod. Dev.* 59, 5–10. <https://doi.org/10.1080/07924259.2014.925516>.
- Snell, T.W., Johnston, R.K., Matthews, A.B., Zhou, H., Gao, M., Skolnick, J., 2018. Repurposed FDA-approved drugs targeting genes influencing aging can extend lifespan and healthspan in rotifers. *Biogerontology* 19, 145–157. <https://doi.org/10.1007/s10522-018-9745-9>.
- Suthers, I.M., Rissik, D., Richardson, A.J., 2019. *Plankton. A Guide to Their Ecology and Monitoring for Water Quality*, Second ed. CRC Press, Florida.
- Varga L., 1966. *Rotifers I*. Hungarian Academy of Sciences, Budapest.
- Venâncio, C., Castro, B.B., Ribeiro, R., Antunes, S.C., Abrantes, N., Soares, A., Lopes, I., 2018. Sensitivity of freshwater species under single and multigenerational exposure to seawater intrusion. *Philos. Trans. R. Soc. B* 374, 20180252. <https://doi.org/10.1098/rstb.2018.0252>.
- Walsh, E.J., Schröder, T., Wallace, R.L., Rico-Martinez, R. 2009. Cryptic speciation in *Lecane bulla* (Monogononta: Rotifera) in Chihuahuan Desert waters. *S.I.L. Proceedings*, 30, 1046–1050. doi:10.1080/03680770.2009.11902298.
- Yamazaki, M., Kisugi, J., Kimura, K., Kamiya, H., Mizuno, D., 1985. Purification of antineoplastic factor from eggs of a sea hare. *FEBS Lett.* 185, 295–298. [https://doi.org/10.1016/0014-5793\(85\)80926-1](https://doi.org/10.1016/0014-5793(85)80926-1).
- Yamazaki, M., Tansho, S., Kisugi, J., Muramoto, K., Kamiya, H., 1989. Purification and characterization of a cytolytic protein from purple fluid of the sea hare, *Dolabella auricularia*. *Chem. Pharm. Bull.* 37, 2179–2182. <https://doi.org/10.1248/cpb.37.2179>.
- Yavuz, B., Chambre, L., Kaplan, D.L., 2019. Extended release formulations using silk proteins for controlled delivery of therapeutics. *Expert. Opin. Drug Deliv.* 16, 741–756. <https://doi.org/10.1080/17425247.2019.1635116>.